

*Examination by
1/23/84
file 9*

REVIEW OF WATERFORD III BASEMAT ANALYSIS

Structural Analysis Division
Department of Nuclear Energy
Brookhaven National Laboratory
Upton, NY 11973

June 21, 1984

8510010634 840621
PDR ADDCK 05000382
E PDR

TABLE OF CONTENTS

	Page No.
INTRODUCTION	1
GENERAL COMMENTS	2
STRUCTURAL ANALYSIS TOPIC REVIEWED	3
1. Dead Loads (D)	3
2. Buoyancy Forces (B)	7
3. Variable Springs Used For the Foundation Modulus	7
4. Vertical Earthquake Effects	8
5. Side Soil Pressure	8
6. Boundary Constraints	10
7. Finite Element Mesh and Its Effect	10
8. BNL Check Calculations	11
CONCLUSIONS AND RECOMMENDATIONS	13
APPENDIX A LIST OF CONTRIBUTORS	A-1
APPENDIX B STRESSES INDUCED WHILE POURING BLOCKS	B-1
APPENDIX C EFFECT OF SIDEWALL LOADS ON BASEMAT CAPACITY	C-1

INTRODUCTION

At the request of SGEB/NRR, the Structural Analysis Division of the Department of Nuclear Energy at BNL undertook a review and evaluation of the HEA Waterford III mat analysis documented in Harstead Engineering Associates (HEA) Reports, Nos. 8304-1 and 8304-2. Both reports are entitled, "Analysis of Cracks and Water Seepage in Foundation Mat". Report 8304-1 is dated September 19, 1983, while Report 8304-2 is dated October 12, 1983. Major topics addressed in the first report are:

- (1) Engineering criteria used in the design, site preparation and construction of the Nuclear Power Island Structure basemat.
- (2) Discussion of cracking and leakage in the basemat.
- (3) Laboratory tests on basemat water and leakage samples.
- (4) Stability calculations for the containment structure.

The second report concentrates on the finite element analysis and its results. Specifically, it describes:

- (1) The geometric criteria and finite element idealization.
- (2) The magnitude and distribution of the loads.
- (3) The final computer results in terms of moments and shear versus the resistance capacity of the mat structure.

Supplemental information to these reports were obtained at meetings held in Bethesda, MD, on March 21 and 26, 1984, at the Waterford Plant site in Louisiana on March 27, 1984, and at Ebasco headquarters in New York City on April 4, 1984. At the close of the EBASCO meeting, a complete listing of the HEA computer run was made available to BNL.

The BNL efforts were concentrated on the review of the results presented in report no. 8302-2 and on the supplemental information contained in the computer run given to us by HEA. This computer run contains 9 load cases and their various combinations. The input/output printout alone consists of roughly two thousand pages of information. Selected portions were reviewed in detail, while the remaining sections were reviewed in lesser detail. Comments regarding the reviewed work are given in the sections that follow.

GENERAL COMMENTS

Basically, the HEA report concludes that large primary moments will produce tension on the bottom surface of the mat. For this condition, it is shown that the design is conservative. Furthermore, the shear capacity vs. the shear produced by load combinations are concluded to be adequate although a few elements were found to be close to the design capacity. Accordingly, the cracking of the top surface is attributed only to "benign" causes such as shrinkage, differential soil settlement, and temperature changes.

Based on the discussions held with EBASCO and HEA, and on the review of data given to BNL, it is our judgement that the bottom reinforcement as well as the mat shear capacity is adequate. The statement that the cracking of the top surface is attributable to "benign" causes however has not been analytically demonstrated by HEA. In the BNL review of the reports and data, an attempt was made to ascertain the reasons for the existing crack patterns that appear around the outside of the reactor shield building as depicted in Figure D-1 Appendix D of the HEA Report 8304-2. Other effects influencing the structural behavior and safety were also investigated. Specifically, the structural analysis topics reviewed in more detail include:

- (1) Dead loads and their effects.
- (2) Buoyancy forces and their effects.
- (3) Variable springs used for the foundation modulus.
- (4) Vertical earthquake effects.
- (5) The side soil pressures.
- (6) The boundary constraint conditions used for the mat.
- (7) Finite element mesh size and its effects.
- (8) BNL check calculations.

STRUCTURAL ANALYSIS TOPICS REVIEWED

1. Dead Loads (D)

As mentioned, EBASCO in their discussion and HEA in their reports have not shown analytically, the cause of the top surface cracks. In reviewing the HEA computer outputs, it was found that element moments and shears for individual loadings are explicitly given. Thus, for the case involving dead loads only, a number of elements in the cracked regions exhibit moments (positive in sign) that can produce tension and thus create cracking on the top surface. This situation is shown in Table 1 which gives moment data (M_x , M_y and M_{xy}) for elements under various load conditions (dead (D), buoyancy (B) and normal side pressure) in some of the cracked regions. The particular elements are also depicted by the shaded areas shown in Fig. 1.

*all
dead
loads
not
just
the one
that
were
up in
77*

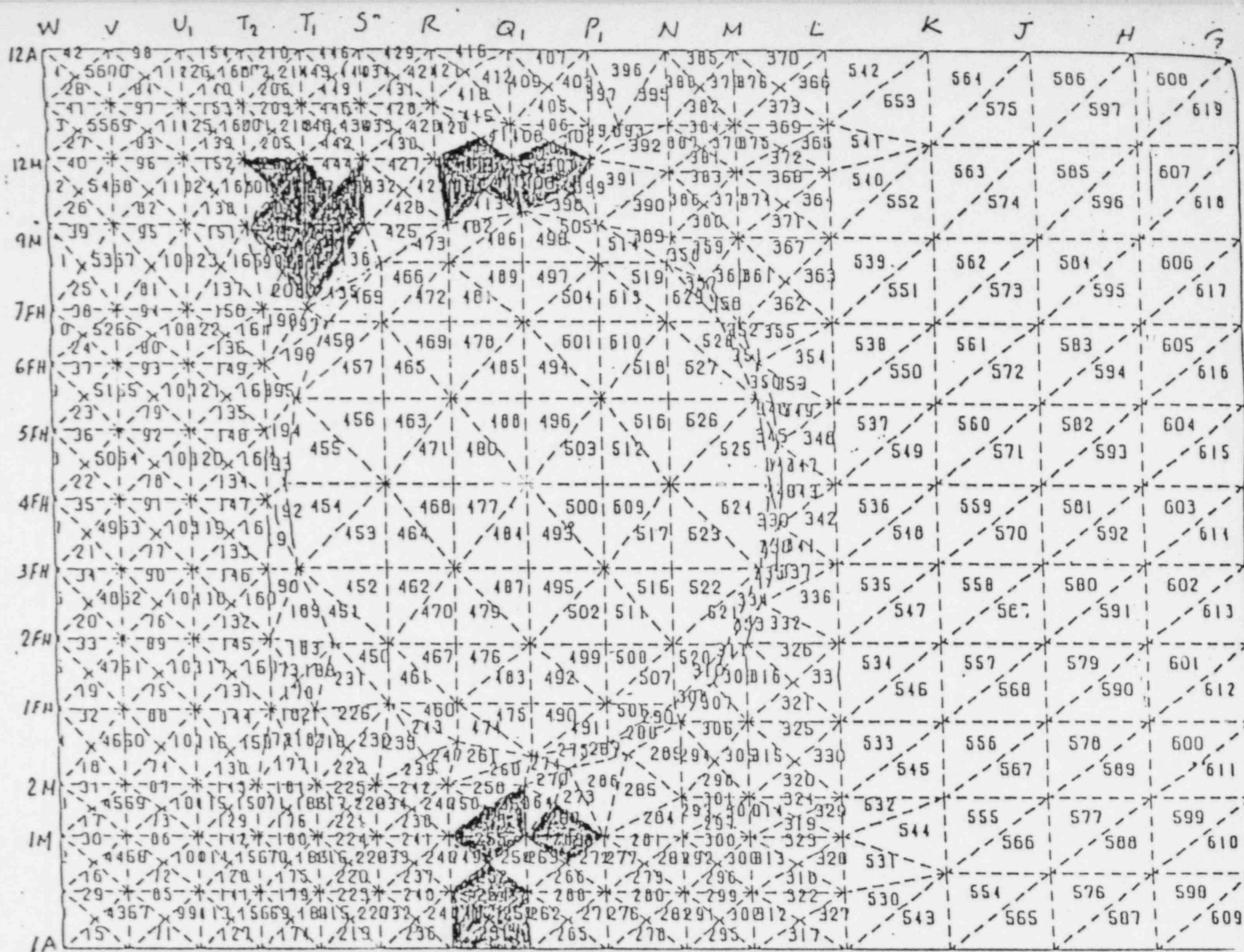
TABLE 1

		Mx (k-ft/ft)		My (kip-ft/ft)		Mxy (kip-ft/ft)		Normal Side Pressure		
ELEMENT		D	B	D	B	D	B	Mx	Mx	Mxy
Area T2-R-12M-7FH	437	-242	173	-574	197	116	- 31	-294	-196	93
	-212	655	595	207	91	106	- 25	-663	-392	79
	211	-605	205	-412	217	-296	48	-219	-416	- 76
	207	64	99	-136	136	- 81	15	-319	-193	50
	441	-105	168	172	-170	39	- 12	-347	-489	66
	436	-719	269	-1193	357	531	-130	-274	-258	117
	438	269	142	-159	158	- 60	26	-730	-347	27
	-447	665	59	210	88	248	- 55	-653	-339	-127
	-204	193	87	569	72	-143	28	-361	-420	24
	-208	350	32	898	- 24	-241	75	-354	-771	- 49
	203	-676	260	-995	236	39	- 21	-574	-247	30
	426	-542	157	-705	310	332	- 65	-171	-486	61
Area R-P-2M-1A	259	62	148	-133	81	154	- 36			
	-253	5	71	531	75	0	18			
	-255	30	58	670	5	41	10			
	252	86	24	611	- 55	87	8			
	254	50	26	412	- 41	69	9			
	251	37	5	162	- 23	44	12			
	-257	320	- 38	57	15	- 81	- 15			
	248	255	- 26	29	16	- 29	- 6			
	267	-236	80	87	118	- 64	28			
	-269	-173	59	434	10	- 82	32			
Area R-P1-12A-9M	419	-314	137	-635	313	- 30	12			
	410	-371	71	-642	238	270	- 29			
	400	-315	108	-774	275	- 44	41			
	401	-180	42	-201	102	108	- 23			
	414	-304	118	-130	178	44	- 19			
	417	-200	93	440	41	- 17	- 15			
	404	- 64	17	428	- 32	98	- 18			

NOTE: D - Dead Load

B - Bouyancy

+ M causes tension at the top surface of the mat.



From the HEA report (page C-2-1-9) it seems that the top reinforcement, which is #11 @ 6" in each direction* is the minimum requirement for temperature steel according to the American Concrete Institute Building Code Specification (i.e., $A_s = .0018 \times 12 \times 144 = 3.11 \text{ in}^2/\text{ft}$). The resisting moment capacity based on working stress design is given by the expression $M = A_s f_s j d$, which can be approximated as $3.12 \times 24 \times 131/12 = \underline{817 \text{ ft-kips/ft}}$. In view of the fact that temperature and shrinkage cracks may exist in the base mat prior to the application of the dead load, the working stress design based on a cracked section used here is considered appropriate.

In checking the data shown in Table 1, it is to be noted for example, that for element 208, the dead load (D) moments M_x and M_y are respectively equal to 350 and 895 ft-kips/ft and are positive. Thus as mentioned previously, the top surface is in tension. The maximum principle moment is a function of M_x , M_y , and M_{xy} and its computed value is close to 1000 kip-ft/ft. This moment exceeds the working stress capacity and thus cracking will occur. Similarly, concrete cracking could occur under the dead load condition in elements 447, 212, 204, 253, 255, 269, 257, 417, and 404. Thus, the cracks on the upper surface outside of the shield wall could have been initiated after construction of the superstructure, before placement of the backfill.

*In a subsequent phone conversation, P.C. Liu of EBASCO stated that some additional reinforcement was added on the top surface in one direction. This was verified in the sketch depicted in Fig. 2 given to BNL by EBASCO where certain areas of the mat are shown strengthened with additional #11 bars are placed every 12 miles in the east west direction.. Even if this is the case the statement that follows is true for the unstrengthened direction and probably even for the strengthened direction.

CLIENT: LOUISIANA POWER & LIGHT CO.

PROJECT: WATKINSFORD 25.3 UNIT NO.3

SUBJECT: COMMON FOR MAT - REIN

DWG NO. _____

DATE _____

CHECKED BY _____

REACTOR PIPE

11020 RW (SHEAR BAR)

11020 RW (SHEAR BAR)

REACTOR PIPE

11020 RW (SHEAR BAR)

11020 RW (SHEAR BAR)

11020 RW (SHEAR BAR)

11020 RW (SHEAR BAR)

11020 RW (SHEAR BAR)

11020 RW (SHEAR BAR)

Fig 2 MAT REINFORCEMENT

In view of the comments made in a later section in this report regarding the finite element grid size and hence, their effects vis-a-vis, the accuracy of the results, an approximate analysis of a strip of the mat was made. This strip was taken at the center of the reactor building in the N-S direction with a width of 22 ft. In this analysis the mat was considered to be infinitely stiff and subjected to the dead loads taken from the HEA computer input. The maximum moment for this case (i.e., 3450 ft-kips/ft) occurs close to the center of the reactor and indeed results in tension on the top surface. This magnitude exceeds the cracking capacity of the mat which is in the neighborhood of 1764 ft-kips/ft. Somewhat lower but similar results would occur at the other cracked sections shown shaded in Fig. 1.

Thus, in summary, the cracking is most probably caused either by dead loads alone or by dead loads acting on elements somewhat weakened due to previous thermal and shrinkage effects. Essentially, for the latter case, the dead load moments would enhance previously existing small and most likely non observable cracks causing them to become larger and hence, observable.

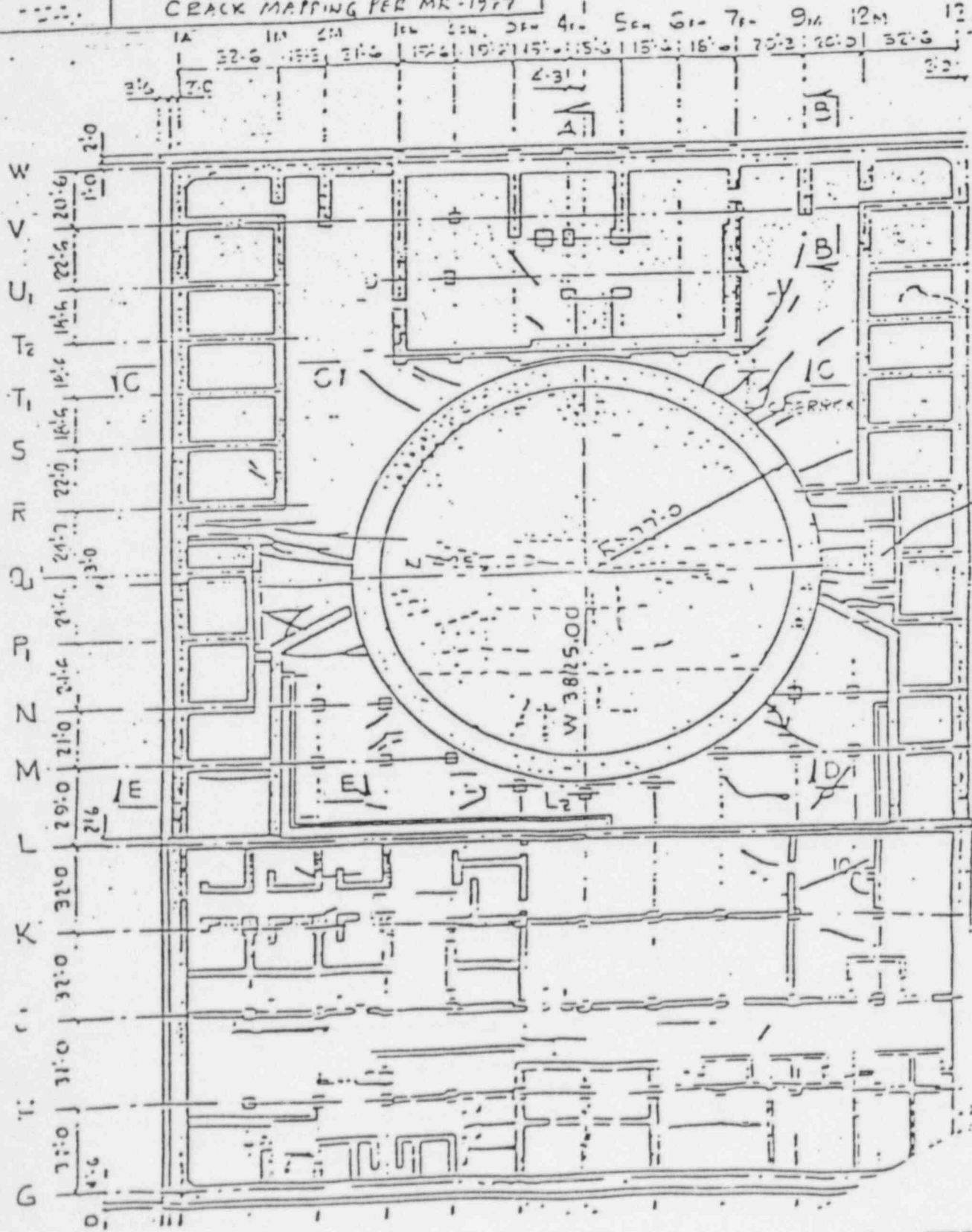
As shown in Table 1 and in Fig. 1, the discussion thus far only pertains to cracks outside of the shield wall. As shown in Fig. 3 crack patterns were also noted in March of 1977, internal to the shield wall. At that time the shield wall was partially constructed up to elevation 187' and the steel containment was supported on temporary footings. Other walls or structures on the mat were either not as yet constructed or were only partially constructed. Since the computer dead load calculations refer to the mat with all existing structures, it is not possible to utilize the computer results to explain the 1977 cracks. It should be pointed out however, that the additional top reinforcements (i.e., # 11 @ 12" shown in Fig. 2) are essentially located in areas under the shield wall and are placed in an east-west direction. Thus, if cracking should occur the preferred direction would

★

Fig. 3 CRACK MAPPING PER
RR/GW 9-21-83 to 9-2-83
for HEA, IOL (A+B)

7A
REACTOR SLOG

CRACK MAPPING PER MR-1977



be parallel to the direction of the heavier reinforcement. This is indeed the direction of the cracks. They could be due to curvature during construction and dead loads acting in conjunction with thermal and shrinkage effects.

The additional east-west direction top reinforcements will also cause prevailing cracks in elements located directly east and west outside of the shield wall circle (i.e., those shown shaded in Fig. 1 in areas R-P-2M-1A and R-P1-12A-9M) to be oriented in an east west direction. This is indeed the pattern indicated in Fig. 3. Since there is no additional top reinforcement in the elements shown shaded in Fig. 1 located between sections T2-R-12-7FH, the prevailing cracks do not necessarily have to be oriented in the east-west direction.

2. Buoyancy Forces (B)

The moment results from this analysis show that these forces when acting alone would mostly cause tensile stress on the upper surfaces. The moments causing these stresses are tabulated in Table 1 under the column heading B for groups of elements in the cracked regions. As can be seen, these moments are not as severe as those due to dead weight. By superposition they could in some cases contribute to higher tensile stresses and thus result in further cracking in some of the upper surface areas.

3. Variable Springs Used for the Foundation Modulus

Moments and shears developed in the basemat were computed using the concept of the Winkler foundation; namely the soil is represented as a series of relatively uniform independent springs. The stiffness of the springs is obtained from approximate analyses which are based on generalized analytical solutions available for rigid mats on the surface of elastic soils. The actual design of the mat was based on a series of iterative computer runs in which the soil stiffness was varied until the computed contact pressures under the mat were fairly uniform and equal to the overburden stress at the eleva-

tion of the foundation mat. This approach appears to be reasonable when assessing the final stress conditions. Long term consolidation effects can be anticipated to cause effective redistribution of loads and cause the mat to behave in a flexible manner. However, during the initial loading stages this approach is not recommended since load redistribution is continuously taking place.

4. Vertical Earthquake Effects

Vertical earthquake effect was not discussed in the HEA reports. However, from the finite element analysis print out and conversation with HEA engineers, it was stated that this effect was included in the load combination cases by specifying an additional factor of 0.067, which was then applied to the dead and equipment load case. From the discussions and the review it is not clear to BNL whether an amplification factor due to vertical mat frequency was used or not.

In order to obtain a rough estimate of this effect, the north-south direction of the mat was simulated by a beam on fourteen elastic supports. The total weight of the mat, the superstructure, the equipment, etc. and the spring constants were the same as those used by Ebasco and HEA in their computer run. The natural frequencies obtained from this analysis are shown below in Table. 2.

Table 2 Natural Frequencies

MODE NUMBER	CIRCULAR FREQUENCY (RAD/SEC)	FREQUENCY (CYCLES/SEC)	PERIOD (SEC)
1	.2863E+02	.4557E+01	.2194E+00
2	.3335E+02	.5305E+01	.1854E+00
3	.3615E+02	.5753E+01	.1738E+00
4	.3721E+02	.5923E+01	.1688E+00
5	.3902E+02	.6210E+01	.1610E+00
6	.4420E+02	.7035E+01	.1422E+00
7	.5031E+02	.8007E+01	.1249E+00
8	.6645E+02	.1058E+02	.9456E-01
9	.8135E+02	.1295E+02	.7724E-01
10	.1112E+03	.1769E+02	.5653E-01
11	.1262E+03	.2009E+02	.4979E-01
12	.1546E+03	.2461E+02	.4064E-01
13	.2041E+03	.3248E+02	.3079E-01
14	.2357E+03	.3752E+02	.2666E-01

As can be seen from the table, the frequencies vary from 4.56 to 37.52, cps. Using Regulatory Guide 1.60, for the 5% damping case, it is found that amplification factors for these frequencies will vary from 3.0 to 1.0. For the first seven frequencies shown in Table 2, the amplification factors will be less than 3.0 but above 2.60. From the review it seems that the vertical amplification factor used by HEA was 1.34, which is below 2.60. It should be realized, however, that not all response parameters (moments, shears, etc.) are sensitive to these frequencies. Moreover, the frequencies were obtained from a simplified model. Hence, to apply an overall amplification factor of say for instance even 2.5 to all response parameters is not reasonable. This situation usually will result in some local effects, such as, increasing the seismic moments at some particular locations. Where this increase occurs is hard to ascertain without performing a very detailed dynamic analysis. Since the effects are localized, it is felt that they should not greatly influence the total resultant stresses acting on the mat.

It should also be realized that the reviewers used Reg. Guide 1.60 to obtain the rough estimates for amplification factors. The guide spectrum is a wide band spectrum that reflects amplifications based on statistical samples of earthquake records. Thus, it is possible that site specific earthquake records could yield lower amplification factors.

5. Side Soil Pressure

According to the STARDYNE computer results obtained from HEA, the normal side soil pressures produce large moments that are opposite to those caused by the dead loads. As shown in Table 1 where moments of elements located in one of the cracked regions outside of the shield building are compared. The total moments in some cases (i.e. element 447 or 208) become quite small. In other regions there is in fact a reversal in the total bending moment which causes tension on the bottom surface and compression on the top. This compression would tend to close the cracks on the upper surface. Thus, it appears that this pressure is a very important load case for the mat design.

For the static or normal operating condition the lateral pressures are based on the at-rest stress condition and are uniform around the periphery of the structure. For the seismic problems the pressures are computed to approximately account for relative movements between the structure and the soil. On one side the structure will move away from soil (active side) and reduce the pressures while the opposite will occur on the other side (passive side). The actual computations made use of site soils properties to arrive at the soil pressures rather than the standard Rankine analyses. No dynamic effects on either the lateral soil or pore pressures was included. The sensitivity of the calculated responses to these effects are currently unknown. However, approximate estimates of these dynamic effects indicate that total lateral load should change by no more than 15 per cent.

6. Boundary Constraints

For equilibrium calculations no special consideration need be made for vertical case since the soil springs prevent unbounded structural motion. However, the same cannot be said for the horizontal case since soil springs are not used to represent the soil reactions. Rather the lateral soil forces are directly input to the model. To prevent unbounded rigid body motion, artificial lateral constraints must be imposed on the model. The constraints are depicted in Fig. 4. The nodes shown circled were constrained from movement in the y direction, while those described by "x" were constrained in the x direction. As commonly practical in finite element applications, the constraints are placed in a manner that they do not overly affect the static and dynamic response calculations. From the output presented in the EBASCO and HEA reports, it is not possible to evaluate the impact of the above shown boundary assumptions. The stresses caused by the artificial boundaries should be calculated and compared with those presented.

7. Finite Element Mesh and its Effects

In general finite element models for plate structures require at least four elements between supports to obtain reasonable results on stress computations. The models used by both EBASCO and HEA violate this "rule of thumb"

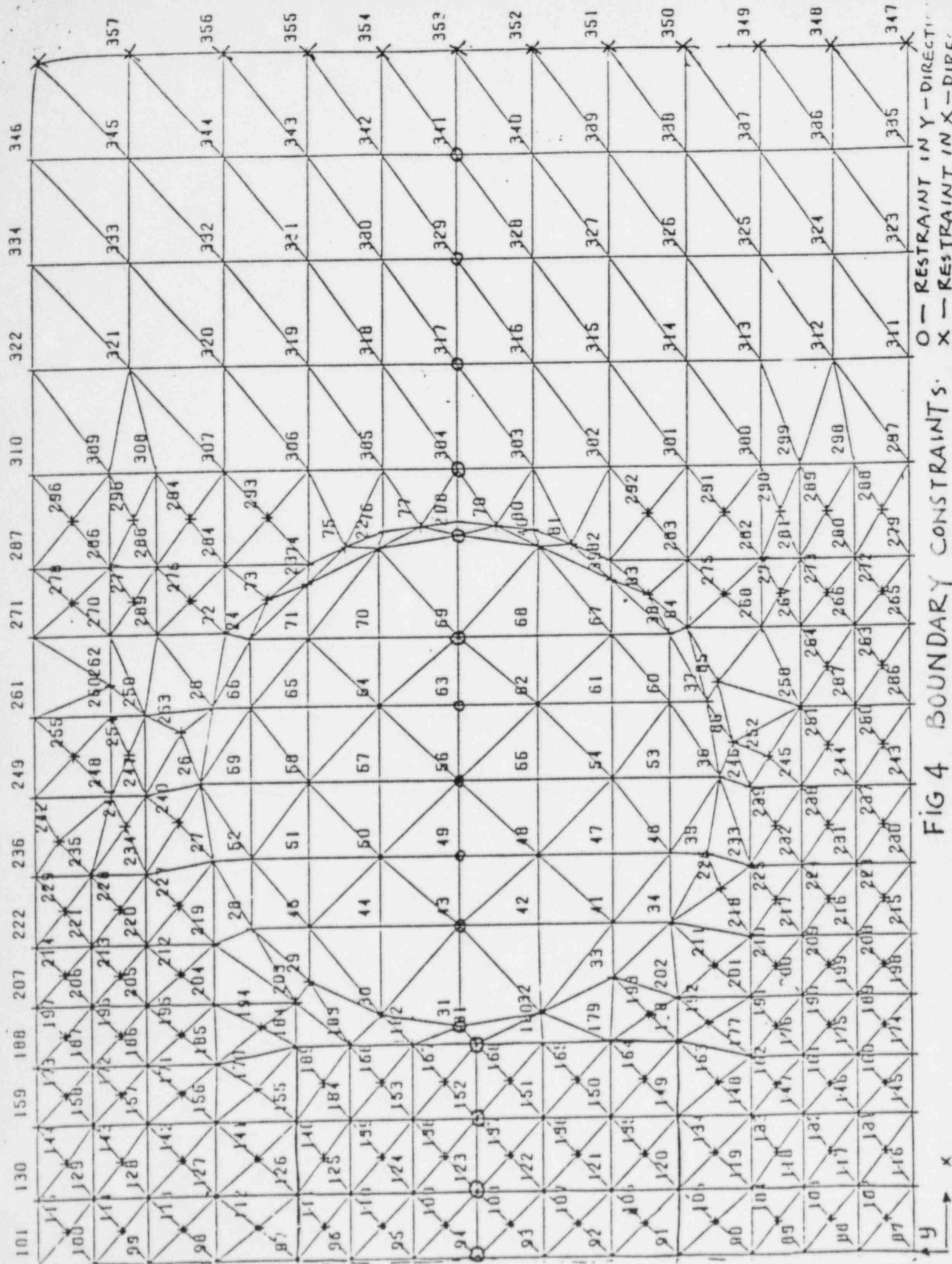


FIG 4 BOUNDARY CONSTRAINTS

O - RESTRAINT IN Y-DIRECT
X - RESTRAINT IN X-DIRECT

in the vicinity of the shield wall. The significance of this effect is demonstrated in Figure D-3 of Report No. 8304-2 which presents a plot of moment taken through the center of the slab. The computed moments in adjacent elements 193, 194 and 455 are -3800, -2500 and +400K. The elements used in the HEA analysis are constant curvature elements so that the computed moments will be constant within each element. The steep moment gradient between the elements indicates that a finer mesh would be advisable. A similar effect was also noted when investigating the elements forming the junction between the lateral earth retaining walls and the base mat.

8. BNL Check Calculations

Due to the questions raised in the items above (4 through 7), it was decided to perform several calculations to verify the acceptability of the mat design.

1. Average Vertical Shear

Several elements in the Ebasco/HEA analysis indicate local areas where allowable shear stresses are exceeded. Shear failure should not be associated with local exceedance of an allowable shear stress. Rather, one should consider the average shear stress across an entire failure plane in the mat. All of the ACI code shear requirements are based on this approach. Two types of average vertical shear stresses (i.e., diagonal tension) were computed in the base mat. The first type considers the average shear through a vertical section across the entire mat (one section in the E-W direction and the other in the N-S direction). These sections were chosen to include those elements which indicated high shear stresses in the HEA analysis and where the actual cracking pattern was noted. The highest average shear stress computed for any design load combination is 50 psi. The allowable shear stress for the case is 107 psi ($2\phi\sqrt{f_c}$). Thus, a safety factor greater than two is available to prevent catastrophic shear failure under the design load combination.

2. Punching Shear

The second type of section considered is a circular punching shear section located a distance of $d/2$ outside the reactor shield wall. The peak value of shear stress due to both SSE overturning moments and normal operating loads (plus proper load factors) were close to but always less than the allowable design shear ($\phi \sqrt{f_c}$).

3. Stresses Resulting From Pouring of Adjacent Mat Blocks

Comments have been made that diagonal tension cracks occurred during the process pouring adjacent mat blocks. To estimate if such cracking is possible an approximate analysis was made. It is included in Appendix B. The adjacent block are assumed to rest on foundation springs which represent the soil flexibility. The second block to be poured was assumed to harden instantaneously thereby overestimating the shear load carried by the first block due to relative settlement of the two blocks. The resulting stresses were found to be sufficiently small so that neither diagonal tension nor bending tensile stresses would be expected to cause cracking. The likelihood of moment cracking was greater than for shear cracking. These conclusions are valid even for the case with soft spots in the foundation where one soil modulus is one half the other.

It should be noted that the soil settlement at the site is found to be instantaneous based on actual measured data. The concrete has almost no strength for the first twelve hours and therefore even the small stresses calculated in Appendix B are unlikely.

(4) Side Loads

Under normal operating conditions the loads acting on the side walls produce an average compressive stress in the base mat of about 50 psi. When seismic loads are included, the average compressive stress in the base mat is about 38 psi. These compressive stresses provide additional shear strength

which have not been included in evaluating the capacity of the mat to carry diagonal tension stresses. It should be noted that the average maximum diagonal tension requirement in the base mat is only 50 psi. Therefore, the potential for the separation of the mat into two halves is unlikely even if a true through crack existed across the entire mat. This analysis is presented in Appendix C.

CONCLUSIONS AND RECOMMENDATIONS

- (a) The Waterford plant is primarily a box-like concrete structure supported on a 12 foot thick continuous concrete mat which houses all Class 1 structures. The plant island is supported by relatively soft overconsolidated soils. To minimize long term settlement effects, the foundation mat was designed on the floating foundation principle. The average contact pressure developed by the weight of the structure is made approximately equal to the existing intergranular stresses developed by the weight of the soil overburden at the level of the bottom of the foundation mat. Thus, net changes in soil stresses due to construction and corresponding settlements can be anticipated to be relatively small.
- (b) In reviewing the information, reports, and computer outputs supplied to BNL by EBASCO, HEA, and LPL, it is concluded that normal engineering practice and procedures used for the analysis of nuclear power plant structures were employed.
- (c) Accepting the information pertaining to loadings, geometries of the structures, material properties and finite element mesh data, it is the judgement of the reviewers that:
 - (i) the bottom reinforcement as well as the shear capacity of the base mat are adequate for the loads considered.

- (ii) the computed dead weight output data can be used to explain some of the mat cracks that appear on the top surface. The cracks that appear, could have occurred after the construction of the superstructure but before the placement of the backfill. Their growth would then be constrained by subsequent backfill soil pressure.
- (d) Due to the existence of the cracks, it is recommended that a surveillance program be instituted to monitor cracks on a regular basis. Furthermore, an alert limit (in terms of amount of cracks, and or crack width, etc) should be specified. If this limit is exceeded, specific structural repairs should be mandated.
- (e) It is also recommended that a program be set up to monitor the water leakage and its chemical content.
- (f) BNL has reviewed the information provided by EBASCO, HEA, and LPL. The following questions concerning their analyses were developed:
 - (i) dynamic coupling in the vertical direction between the reactor building and the base mat.
 - (ii) dynamic effects of lateral soil/water loadings.
 - (iii) artificial boundary constraints in finite elements models.
 - (iv) fineness of base mat mesh.

Based upon our approximate calculations together with engineering judgment, we do not anticipate that the above questions will lead to major changes in calculated stress levels. Thus, it is our opinion that the safety margins in the design of the base mat are adequate. However, it is recommended that some detailed confirmatory calculations be performed in the near future to strengthen the above conclusions.

APPENDIX A-1
LIST OF CONTRIBUTORS

Listed below in alphabetical order are the names of the contributors to this report:

Costantino, C.J.
Miller, C.A.
Philippacopoulos, A.J.
Reich, M.
Sharma, S.
Wang, P.C.

Appendix B

Stresses Induced While Pouring Blocks

A question has been raised concerning the stresses which could have been introduced when the basemat blocks were being poured. The response of two adjacent blocks during construction are considered. The first block is taken to be in place when the second block is placed. It is also assumed that the concrete in the second block hardens immediately so that it can transmit loads to the first block. The subgrade modulus under the two blocks is assumed to be different so that the effect of soft spots in the soil can be considered. A sketch of the problem to be considered is shown in Fig. 1.

When the first block is poured it settles an amount,

$$\Delta_1 = W/K_1$$

The second block is then poured. If the concrete is conservatively assumed to harden before the soil settlement can occur, the second block will introduce additional loadings on the first block. The new deformation caused by the weight of the second block is shown on Fig. 2.

The loads acting on the block may then be determined by multiplying the deformations by the foundation moduli. These loads are shown on Fig. 3. Force and moment equilibrium allow the two unknown displacements (Δ_2) to be calculated. The results are,

$$\Delta_2 = W [(7 + \Omega)/(1 + 14\Omega + \Omega^2)]/K_1$$

$$M = 12 W/[L K_1 (1 + 14\Omega + \Omega^2)]$$

$$\text{where, } \Omega = K_2/K_1$$

Once the displacements are known the loads on the blocks may be evaluated and beam shears and bending moments may be computed. This is done for foundation moduli ratios of 1, 0.5, and 0. Peak values of shear and moment are tabulated in Table 1.

Table 1

Shear and Moments in Blocks During Construction

Foundation Moduli Ratio (Ω)	Maximum		Required f'_c (psi) To Prevent	
	Shear (Kips)	Moment (Kip-ft)	Shear Failure	Bending Tension Crack
1	563	5040	15	15
0.5	819	13770	31	113
0	4689	156375	1091	14559

For the design concrete strength of 4000 psi, the shear capacity of the concrete section is 9290 kips. As may be seen this is much larger than the peak shears that could be caused during construction. Bending cracks will occur in the concrete when the peak concrete tensile stress reaches the modulus of rupture. For the concrete design strength this will occur at a bending moment of 81966 kip-feet. It may be seen that the peak moments are closer to the value required to cause a bending crack than the peak shears are to that required to cause a diagonal tension crack.

The concrete will not have attained its final strength at the time when these stresses occur. The last two columns in Table 1 list the required concrete compressive strength to prevent shear and moment failures. Two conclusions may be drawn from these data. First, even for rather dramatic variations in foundation moduli, only a minimal concrete strength is required to prevent either a shear or moment crack. Second, if a crack were to develop it would most likely be a bending crack.

The above analysis is based on the assumption that the concrete hardens before soil settlement occurs. If this were not so, the wet concrete would

fill the void volume created by soil settlement. The concrete block would then be supported on the soil rather than "hanging" from the other block. Figure 4 shows the concrete strength gain during the first day. As may be seen concrete will have no strength until about 12 hours. By this time all of the soil settlement would have occurred and the second concrete block would not induce any loads on the first block.

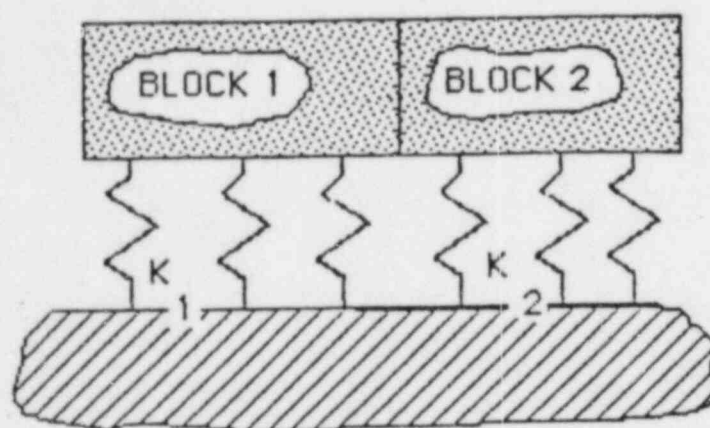


Fig. 1 Construction of Two Adjacent Blocks

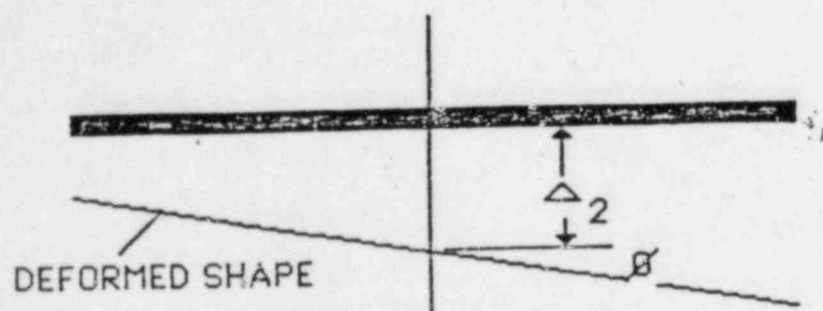


Fig. 2 Deformed Shape of Blocks

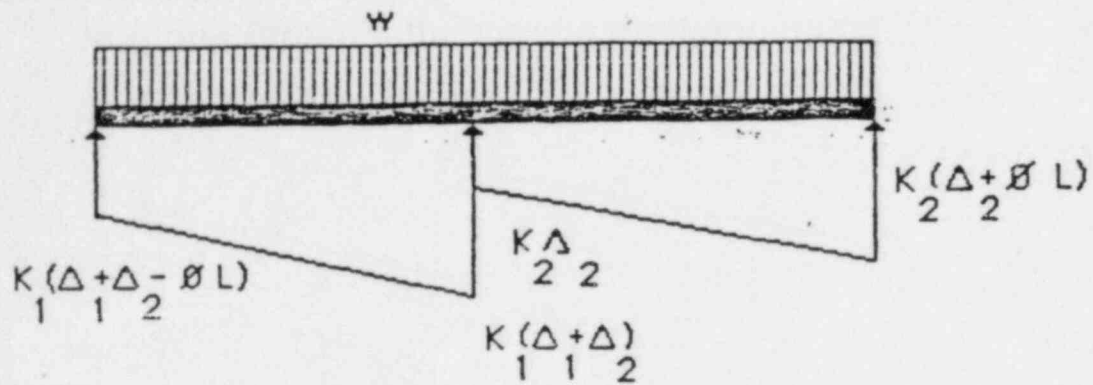


Fig. 3 Loads Acting on Blocks

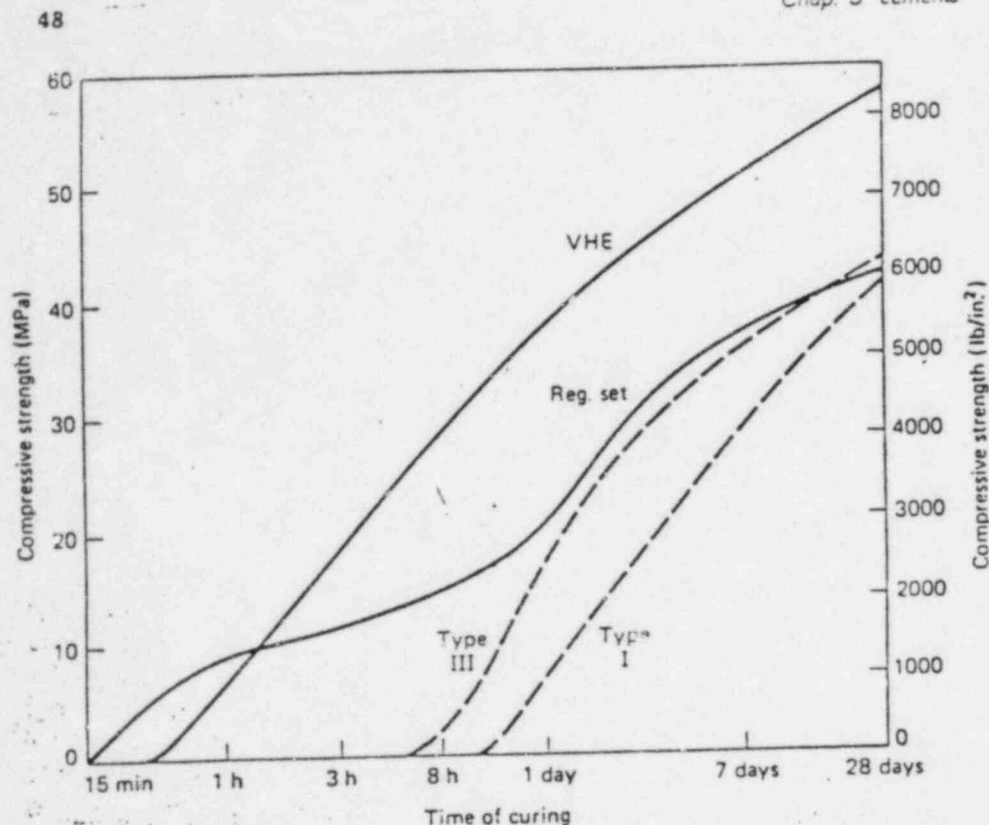


Figure 3.13 Strength developments of concretes made with rapid-hardening cements. (Adapted from W. Perenchio, in *New Materials in Concrete Construction*, ed. S. P. Shah, University of Illinois at Chicago Circle, Chicago, 1972, p. 12-VI.)

placement and have the advantage of better water resistance. But the very rapid strength gain of the cement suggests many other applications in which the properties of a portland cement are desired: pavement and bridge-deck repair, precasting operations, shotcreteing, and slip forming. It is unfortunate that regulated-set cement is not currently available in the U.S., but the interesting properties of the cement will no doubt ensure its reappearance.

VHE Cement

In the production of VHE cement, calcium sulfate is added to the raw mix so that $C_4A_3\bar{S}$ is formed in the rotary kiln. This is the same compound that is present in Type K expansive cements, but the quantities are greater in VHE cement. Calcium sulfate ($C\bar{S}$, insoluble anhy-

Appendix C

Effect of Sidewall Loads On Basemat Capacity

Soil pressure loads act on the sidewalls and these loads introduce compressive stresses in the slab of the basemat. This compressive stress will assist in resisting the diagonal tension stresses which occur in the slab. The significance of this effect is discussed in the Appendix.

Table B.1 lists the horizontal loads which act on the sidewalls due to the various load combinations. These loads were determined directly from the HEA/Ebasco computer printouts. An elevation of the structure parallel to the long direction of the basemat is shown on Fig. B.1. The forces (P) are taken as the forces shown on Table B.1 and acting on walls #2 and #4. The soil pressure is assumed to have a triangular variation as shown so that the resultant force (P) acts at the third point on the wall. Since the wall is buried about 54', the resultant force acts at a point 18' up the wall from the bottom of the basemat.

The stresses caused by this loading in the cross section shown on Fig. B.2. The basemat is analyzed as a beam structure. The cross section shown in Fig. B.2 has the following properties:

Cross sectional area = 3552 square feet
 Centroid at 7.91' above the bottom of the mat
 Moment of inertia = 247300 feet⁴

Stresses are then computed as:

$$f = P/A \pm Mz / I$$

Therefore at the top of the wall,

$$f_{tw} = P/3552 + P (18-7.91) (54-7.91) / 247300$$

The stress at the top of the slab is,

$$f_{ts} = P/3552 + P (18-7.91) (12-7.91) / 247300$$

The stress at the bottom of the slab is,

$$f_{bs} = P/3552 - P (18-7.91) (7.91) / 247300$$

The resultant stresses for the Case 4 loads (Normal soil pressure) are:

$$f_{tw} = 541 \text{ psi}$$

$$f_{ts} = 112 \text{ psi}$$

$$f_{bs} = -11 \text{ psi}$$

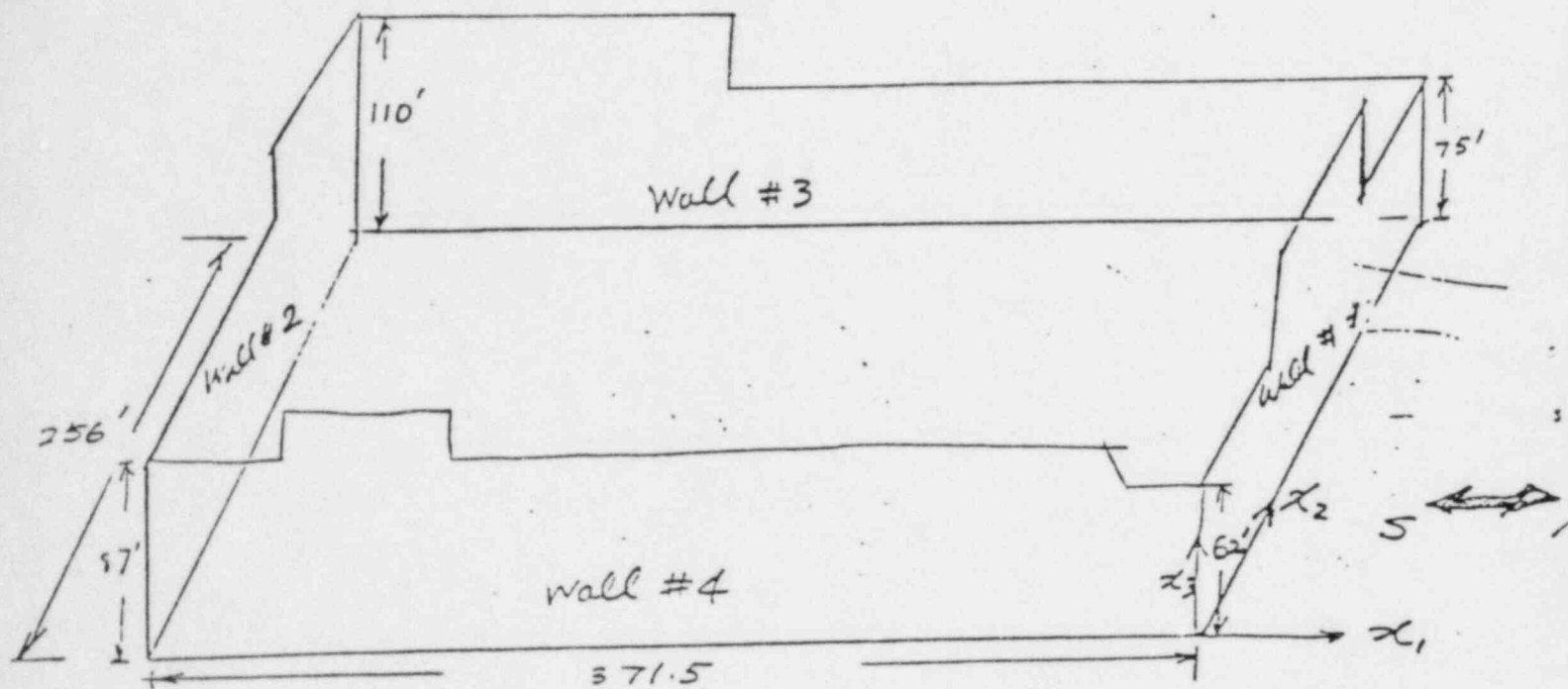
The stresses for Case #8 (SSE in N-S) are:

$$f_{tw} = 465 \text{ psi}$$

$$f_{ts} = 84 \text{ psi}$$

$$f_{bs} = -8 \text{ psi}$$

The average stresses in the slab for these two load cases are 51 psi and 38 psi respectively. The average shear in the basemat for Case 8 loadings was found to be 50 psi. If this shear stress is combined with the 38 psi average compressive stress one finds that the tensile stress in the concrete is reduced to 34 psi. It is unlikely that this stress could cause a shear (diagonal tension) failure.



Total Force Acting on the Wall Surface (kips)

Load Case	Wall #1	#2	#3	#4
Case 4: Normal Soil Pressure	36619	36441	50942	50522
Case 8: SSE & Soil (North to South)	27061	110657	50684	50377
Case 10: SSE & Soil (South to North)	111051	26907	50684	50377

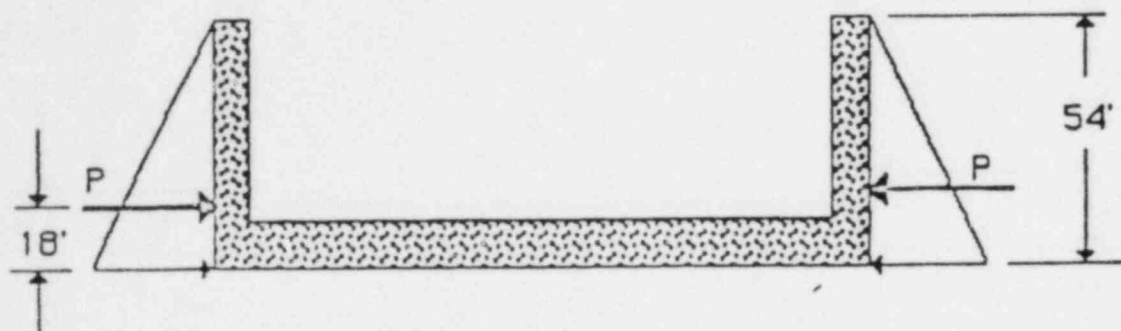


Fig. 1 Estimated Side Loads On Wall

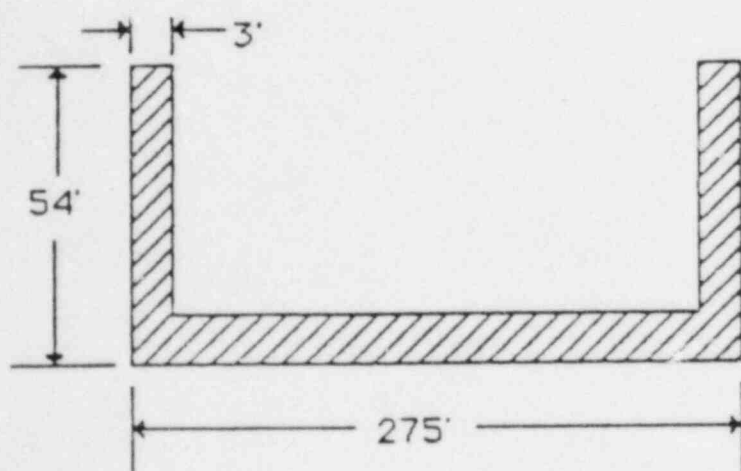


Fig. 2 Cross Section of Basement